

Regime Rays: Visualizing the Fermat/Snell Loci in Homogeneous Anisotropic Media

William J. Vetter, P.Eng. (NF), Ph.D., (ret. Prof. Eng., Memorial U., NF Canada)

vetterb@sympatico.ca Kitchener, ON

Summary

Present understanding and analytical encapsulation of anisotropy kinematics, even in homogeneous anisotropy medium segments which are here the focus, is incomplete/incorrect re the familiar Fermat/Snell ray theory premises [-> *FS-rays*]. The travelttime expression $t_{ON} = t_{OE} = (r_E \bullet n_N) / v_N(n_N, c_{ij}, \rho)$, attributed to Green (Love 1927, Rudzki 1911), has been deemed essentially a mode-specific plane-wave progression dictate [here O, N, E subscripts designate Origin, front-Normal points/directions, Energy-flux arrival- points/directions]. It is moreso a constraint, call it an *ansatz* (starting premise), which for particular homogeneous anisotropic medium models and specified front-normal direction firms direction/progression-speed of *FS-ray* segmentals in part along front-normal direction but, it turns out, with complementing segmentals with maximally two other orientations. *Regime rays* is label for representation loci, when like-oriented segmentals have been re-ordered to single segments, and those segments are then linked.

Through *regime rays* we can discern and quantify significant analytical *FS-rays* detail, the time-fractions and segment lengths plus progression speeds for the three or fewer oriented segments. Those details yield the significant *FS-ray*-specific characterizing velocities for the along-paths velocity distributions $\{v_{APPARENT}, v_{TIME-AVE}, v_{RMS}, v_{PATH-MEAN}\}$; also l_{PATH} which are true pathlengths for intangible *FS-ray* loci.

All this comes from overlooked extra prescribed directions/progression-speeds detail in sequenced mode-relevant eikonal equations, relevant for *FS-rays* for given front-normal directions. The *FS-rays* per se, say in medium natural coordinate frame, progressing mode-specific from point-shots r_O at origin to r_E -front-points, are anchored to their energy flux line-loci, the 'so-called *group-* or *ray-*velocity representation loci'. Beyond analytical essentials previously communicated I provide here simulations/ visualization for all modes of an orthorhombic standard model. *Regime rays* clarify the long-puzzling detail between paired points on the wave surfaces and their *ansatz*-front-normal velocity representation surfaces.

From travelttime *ansatz* to *regime rays* models

It is well established that wave propagation disturbances through composites of fine-structured layering and fine-structured heterogeneities broadly, have EMT (effective medium theory, long wavelength regime) progression speeds that are virtually constant beyond a distinct transition zone re wavelength/composites-repetition-thickness ratio (e.g. Macbeth 2002). I suggest that Fermat's principle and Snell's law should apply in such composites also for long wavelength regime *FS-rays*, for progression directions not just orthogonal or parallel to ordered layering or other fine-scale structured heterogeneity. This can be credibly expected, because in the broader physics context Snell's law and Fermat's principle are encompassed within the remarkable '*principle of least action*' of Maupertuis [1746], [also Leibniz, Euler, Hamilton, Feynman,...]. At any rate, what manifests from this hypothesis agrees with analytical models and kinematics manifestations in diverse experiments. As simplest example take the above pathtime *ansatz*

$t_{ON} = t_{OE} = (\mathbf{r}_E \bullet \mathbf{n}_N) / v_N(\mathbf{n}_N, c_{ij}, \rho)$, but reduced to progression paths in just the x-vs.z plane as $t_{ON} = t_{OE} = (x_E \sin\theta + z_E \cos\theta) / v_N$, with θ as polar angle re z-axis direction. Then if $x_E > z_E \tan\theta$, the as two segments partitioned equivalent is $t_{ON} = t_{OE} = (z_E / \cos\theta) / v_N + (x - z_E \tan\theta) / (v_N / \sin\theta)$. First segment has length $l_1 = (z_E / \cos\theta)$ with progression speed $v_1 = v_N$, and the second $l_2 = (x - z_E \tan\theta)$ with speed $v_2 = (v_N / \sin\theta) > v_N$. Transition $v_1 = v_N$ to $v_2 = v_N / \sin\theta$ conforms with Snell's law, front-normal oriented l_1 of *regime ray* in y=0 plane refracting into x-direction oriented l_2 , ending at front point $[x_E \ z_E]$.

Else if $z_E \tan\theta > x_E$, the *ansatz* transforms to $t_{ON} = t_{OE} = (x_E / \sin\theta) / v_N + (z_E - x_E / \tan\theta) / (v_N / \cos\theta)$, with $l_1 = (x_E / \sin\theta)$ and speed $v_1 = v_N$ front-normal oriented. Then Snell's law conforming refraction produces z-directed $l_2 = (z_E - x_E / \tan\theta)$ with $v_2 = (v_N / \cos\theta) > v_N$, ending at $[x_E \ z_E]$ front-point.

The common pathtime *ansatz* expression has been reframed in two ways, depending on specific association detail between front-normal orientations and for given medium parameters consequent energy flux loci (so-called ray- or group-velocity representation loci), both with two-segmented *regime ray* components.

The general *ansatz* can/must be elaborated to one of 18 different expanded detail forms [really 25, of which 7 have single-direction loci]. *Regime rays* are analytical representations for the significant *FS-rays* detail, through aggregation of same-oriented segmentals to single segments. The *regime rays* condense unknown detail re sequenced segmentals into analytical expressions which reveal then essence of that detail. Much of that analytical detail is can be found in a previous Abstract (Vetter 2007, accessible through CSEG: '2007 CSPG CSEG Joint Convention', Seismic Processing II).

Orthorhombic Medium Simulation Example

Figures 1 to 3 below show *regime rays* simulation detail for Schoenberg and Helbig's (1997) 'orthorhombic standard model'. I have used Helbig's explicit Kelvin-Christoffel matrix expansion (1994, Appendix 4B, short version valid for orthorhombic and higher symmetry in medium natural coordinate frame), and a novel compact expression for vectored \mathbf{r}_E , derived from the pathtime ansatz [(eqn 1b) in spherical coordinates (θ, ϕ)], together with the pathtime minimizing derivatives re (θ, ϕ) . The below equation 2 is its column-vectored form, after re-converting from spherical- back to rectangular coordinates.

As an important 'aside', eqn.2, columned as shown, is variously incorrect in the literature [e.g. Helbig 1994, p.13 eqn.1a.6{without common dispersion term}; Mensch and Rasolofosaon 1997 eqn.12; ...]. Further, Auld's (1973) suggested 'carrier modulation' analogy, [velocity of carrier<--> vectored *phase velocity*, velocity of modulation envelop<--> vectored *group- or ray- velocity*] is not realistic/ applicable, nor are then 'phase-' and 'group-velocity' really relevant or proper designations for context of the *FS-rays ansatz*.

Equation (3), also from eqn.1b plus derivatives, is important for visualization, transparency, and credibility of the *regime rays*, which reveal pathtimes/ pathlengths/ velocity detail, and thus quantifiable heterogeneity.

$$t_{ON} = t_{OE} = (\mathbf{r}_E \bullet \mathbf{n}_N) / v_N(\mathbf{n}_N, c_{ij}, \rho) = (x \sin\theta \cos\phi + y \sin\theta \sin\phi + z \cos\theta) / v_N(\theta, \phi; c_{ij}, \rho) \quad (1a, 1b)$$

$$\begin{pmatrix} \frac{x}{t} \\ \frac{y}{t} \\ \frac{z}{t} \end{pmatrix} = \begin{pmatrix} n_x \\ n_y \\ n_z \end{pmatrix} * v_N + \begin{pmatrix} 1 - n_x^2 & -n_x n_y & -n_x n_z \\ -n_x n_y & 1 - n_y^2 & -n_y n_z \\ -n_x n_z & -n_y n_z & 1 - n_z^2 \end{pmatrix} \begin{pmatrix} \frac{\partial v_N}{\partial n_x} \\ \frac{\partial v_N}{\partial n_y} \\ \frac{\partial v_N}{\partial n_z} \end{pmatrix}; \quad \mathbf{n}_N = [n_x \ n_y \ n_z] \quad (2)$$

$$\left(\frac{x}{t}\right)^2 + \left(\frac{y}{t}\right)^2 + \left(\frac{z}{t}\right)^2 = v_E^2 = v_N^2 + \left(\frac{\partial v_N}{\partial \theta}\right)^2 + \left(\frac{1}{\sin\theta} \frac{\partial v_N}{\partial \phi}\right)^2 = v_N^2 + \left(\sqrt{\left(\frac{\partial v_N}{\partial \theta}\right)^2 + \left(\frac{1}{\sin\theta} \frac{\partial v_N}{\partial \phi}\right)^2}\right)^2 \quad (3)$$

Six *regime rays* are simulated for qP-, qSV- and qSH-modes, from origin to cross-diagonal between $[x\ y\ z] = [3\ 0\ 0] \rightarrow [0\ 3\ 3]$, for equi-angle stepped front-normals. This sampling shows changes from near-surface in-layers-dominant to deeper cross-layers and at-slant-encountered cracks. The displays are km-spatial, with progression SPEEDS made tangible through dot-density [40 intervals per second]; DENSE is slow and SPARSE is fast! The action per se is virtually on the energy flux loci from **Origin** to **E** shown in **RED**, but detail is visualized through *regime ray* segments; fine-dots red link the **E**-points. Front-normal **N**-points and dotted *regime rays* are **BLUE**; fine-dots-blue link the **N**-points. The **GREEN**-framed **R-E-N** triangles are tangent plane portions anchored at **E**, with pythagoras **Right angle points** linking to 2nd segments extended.

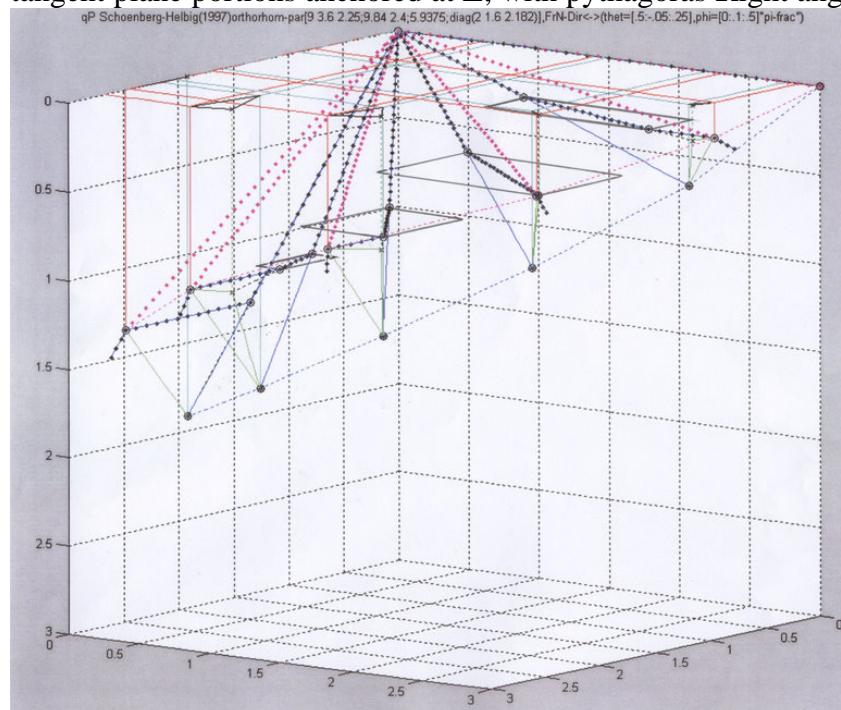


Fig.1: qP-mode *REGIME RAYS*

Schoenberg-Helbig orthorhombic model

Data for # 2 & # 4 FS-rays

# 2	directions	time	length	velo
E[.	9627 . 2619 . 0674]	1.000	2.9670	2.9670
N[.	9393 . 3052 . 1564]	.4328	1.2775	2.9516
Z[.	9511 . 3090 0]	.4192	1.2526	2.9884
x[1.0000 0 0]	.1480	.4652	3.1422
	vTA=2.9953	vRMS=2.9959	vPM=2.9966	
	lenPATH=2.9953		vN=2.9516	
P[.	9574 . 2757 . 0860]	Polarization _____		
# 4	directions	time	length	velo
E[.	4817 . 5837 . 1577]	1.000	2.9101	2.9101
N[.	5237 . 7208 . 4540]	.5832	1.6514	2.8316
Z[.	5878 . 8090 0]	.2874	.9133	3.1780
y[0 1.0000 0]	.1294	.5083	3.9282
	vTA=3.0730	vRMS=3.0944	vPM=3.1159	
	lenPATH=3.0730		vN=2.8316	
P[.	5010 . 8097 . 3056]	Polarization _____		

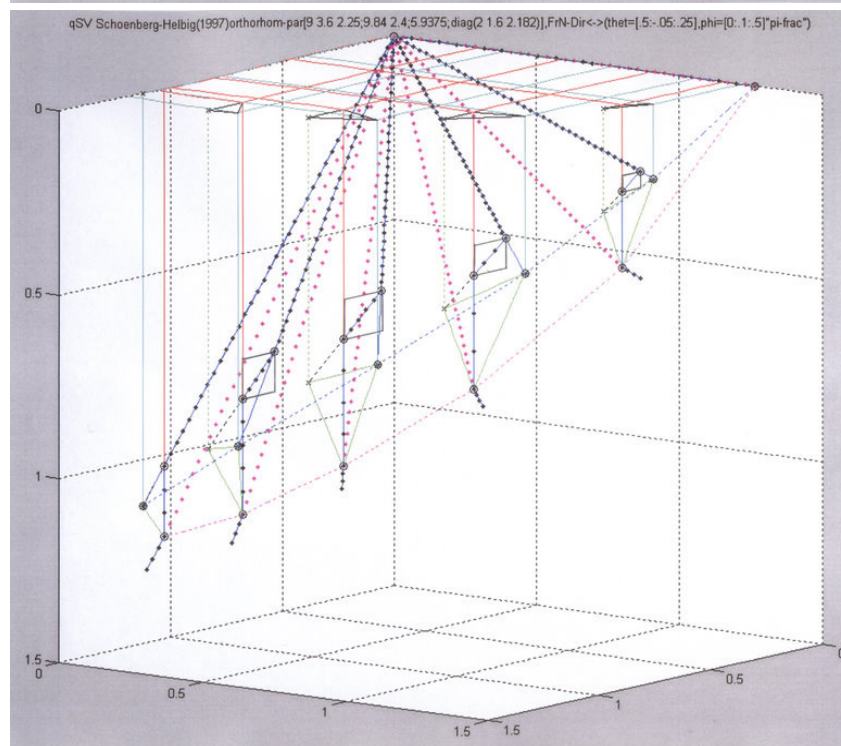


Fig.2: qSV-mode *REGIME RAYS*

Schoenberg-Helbig orthorhombic model

Data for # 2 & # 4 FS-rays

# 2	directions	time	length	velo
E[.	8757 . 3485 . 3342]	1.000	1.3243	1.3243
N[.	9393 . 3052 . 1564]	.9501	1.2346	1.2995
X[0 . 3053 . 1564]	.0251	.0952	3.7889
z[0 0 1.000]	.0248	.2061	8.3067
	vTA=1.5359	vRMS=1.9175	vPM=2.3939	
	lenPATH=1.5359		vN=1.2995	
P[-.	0652 -. 0838 . 9943]	Polarization _____		
# 4	directions	time	length	velo
E[.	3946 . 6566 . 6427]	1.000	1.5100	1.5100
N[.	5237 . 7208 . 4540]	.7753	1.1377	1.4674
X[0 . 8462 . 5329]	.1176	.2025	1.7225
z[0 0 1.0000]	.1071	.3460	3.2322
	vTA=1.6863	vRMS=1.7711	vPM=1.8602	
	lenPATH=1.6863		vN=1.4674	
P[-.	2033 -. 2331 . 9510]	Polarization _____		

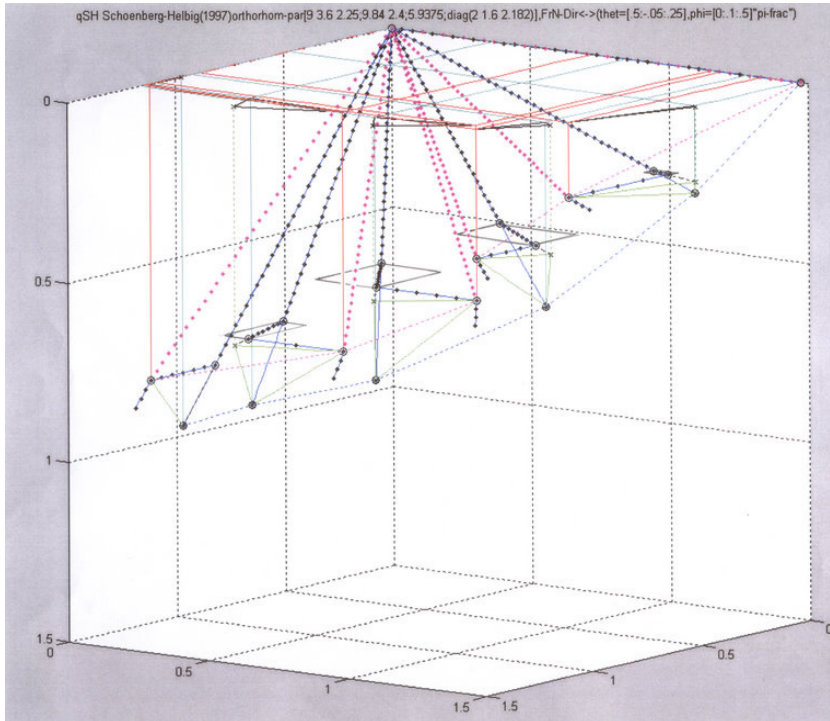


Fig.3: qSH-mode *REGIME RAYS*

Schoenberg-Helbig orthorhombic model

Data for # 2 & # 4 *FS-rays*

# 2	directions	time	length	velo
<u>E]. 8236 . 5520 . 1302]</u>		1.000	1.6154	1.6154
N[. 9393 . 3052 . 1564]		.8647	1.3445	1.5548
Z[. 9511 . 3090 0]		.0451	.0711	1.5742
y[0 1.0000 0]		.0902	.4595	5.0942
vTA=1.8749 vRMS=2.1314 vPM=2.4229				
lenPATH=1.8749 vN=1.5548				
P[-. 2814 . 9576 . 0623] Polarization_____				
# 4	directions	time	length	velo
<u>E]. 6945 . 6568 . 2938]</u>		1.000	1.6571	1.6571
N[. 5237 . 7208 . 4540]		.6668	1.0724	1.6083
Z[. 5878 . 8090 0]		.2160	.3898	1.8050
x[1.0000 0 0]		.1172	.3601	3.0709
vTA=1.8222 vRMS=1.8799 vPM=1.9393				
lenPATH=1.8222 vN=1.6083				
P[-. 8412 . 5386 -. 0479] Polarization_____				

Focus initially on Fig.3 qSH-mode with its #2 *regime ray* and the boxed data. E-rowed underlined data is for red-dotted energy flux locus, so-called *group-* or *ray-*(velocity) representation. {N Z y} is code for regime ray segment orientations, here N for 3D front-normal, Z for in parallel to coordinate frame z-plane, and y for y-axis parallel. Segment 2 looks like a blur, but details the boundary of small z-plane rectangle with segment progressing diagonally; c.f. outlined plane areas for second segments of other *regime rays*. Note regime changed to {N Z x} for #4 *regime ray*, which through nearness of #3 and #4 energy flux loci suggests a ‘flip-point’, possibly even a cusping-like swerving. Attentive readers will notice and ponder the distinctly different *regime rays* patterns for the different modes; e.g. shear-modes *horizontal/ vertical* have second and third *regime ray* segments so-oriented. And remarkably FAST can manifest for third segments!

Conclusions

Regime rays encapsulate and quantify the fine structured anisotropic medium heterogeneity encountered along wave disturbance energy-transport channels through their significant direction and propagation speed detail. Because that detail links to parameters of relevant elastic medium models, they will be important for seismic wave propagation-, and particularly for anisotropy velocity field- modeling, as also potentially for data to-medium-models inverting. I expect *regime rays* will bring anisotropy kinematics back into the *FS-ray theory* purview, however with minor refinement of its premises.

References

Auld, B. A., 1973, *Acoustic Fields and Waves in Solids*, vol. I: John Wiley and Sons.

Cerveny, V. 2001, *Seismic Ray Theory*: Cambridge University Press.

Helbig, K., 1994, *Foundations of Anisotropy for Exploration Seismics*: Pergamon

Love, A.E.H., 1927, *A Treatise on the Mathematical Theory of Elasticity*: (1944 Dover republ. of 4th ed. Cambridge U. Press)

Macbeth, C., 2002, *Multi-Component VSP Analysis for Applied Seismic Anisotropy*: Pergamon.

Mensch, T., Rasolofosaon, P., 1997, Elastic-wave velocities in anisotropic media ...: *Geophysics Journal Internat*, **128**, 43-64.

Rudzki, M.P., 1911, Parametrische Darstellung der elastischen Wellen in anisotropen Medien, *Bulletin Academie Cracovie* 503-536 (Parametric representation of elastic waves in anisotropic media).

Schoenberg, M., Helbig, K., 1997, Orthorhombic media: Modeling elastic wave behavior in ... *Geophysics*, **62**, 1954-1974.

Vetter, W. J., 1993, The Fermat path ... in anisotropic media: 63rd Annual Intern. Meeting, SEG, Expanded Abstract, 953-956.

Vetter, W. J., 2007, Anisotropy Kinematics Clarified though Regime Rays Model: 2007 CSPG CSEG Convention, 563-567.